Measuring the evolution of early-type galaxies in GAMA using observationally robust quantities

Rongfu Liu, Alessandro Sonnenfeld

Accepted XXX. Received YYY; in original form ZZZ

ABSTRACT

test This is a simple template for authors to write new MNRAS papers. The abstract should briefly describe the aims, methods, and main results of the paper. It should be a single paragraph not more than 250 words (200 words for Letters). No references should appear in the abstract.

Key words: keyword1 – keyword2 – keyword3

1 INTRODUCTION

Early type galaxies (ETGs) ,which are typically elliptical in shape, are believed to be passively evolved after their star-forming activities being quenched. Over the past few decades, observations have confirmed that the ETGs at the epoch of $z \approx 2$ are much more compact than their counterpart at $z \approx 0$ (Daddi et al. (2005), Toft et al. (2007), Trujillo et al. (2006), Trujillo et al. (2007), van Dokkum et al. (2008)). These ultra-compact objects then experienced a dramatic growth in size, in particular, by about a factor of 3 between $z = 2$ and $z = 0$(Damjanov et al. (2019); Fan et al. (2008); Hamadouche et al. (2022); van der Wel et al. (2014); van Dokkum et al. (2010)). Numerous works in literature have confirmed that the dissipationless dry mergers is the major mechanism that attribute to that rapid size growth. (e.g. Naab et al. (2009),van Dokkum & Brammer (2010), Oser et al. (2011),Newman et al. (2012), Hilz et al. (2013), Dekel & Burkert (2014), D'Eugenio et al. (2023)), especially for mergers with mass ratio around 1:10(Newman et al. (2012); Belli et al. (2015)). However, purely minor merger is not sufficient to explain the entire growth , or the number of mergers will be too large in that case(Hopkins et al. (2010); Nipoti et al. (2009)) while the constrain placed by the density slope of galaxies cannot be satisfied (Sonnenfeld et al. (2014)). Some other mechanisms or observational effects must be taken into consideration, such as dry mergers with higher mass ratio (major merger) and the existence of the color gradient.

At relatively lower redshift, newly queched galaxies may join the population of quiescent galaxies. These "fresh blood" of quiescent population are relatively larger, thus could mimic the growth in size of such galaxies.This effect is called "progenitor bias"(Dokkum & Franx (1996); Carollo et al. (2013); Fagioli et al. (2016); van Dokkum & Franx (2001)), and it is also an important effect that may contribute to the observed size evolution of ETGs. Each of these effect will leave impact on some other observable properties of galaxy, such as velocity dispersion, number density and mass, while these impact could in turn place constrains on the effects above. Nevertheless, a theoretical model that could meet all these constrains is still in absence.

Besides, another systematic might be ignored in the literature.The problem arise from the finite photometric depth of observations. it is hard to measure the total light directly (Tal & van Dokkum (2011)) as the information where the surface brightness of galaxies drops below the observation limit remains unknown. To obtain a accurate measurement of the total light, a precise sky-subtraction is demanded while it is easy to bring additional systematic. In literature, we use various models to fit the surface brightness distribution of galaxies . The faint outskirt of galaxies could not provide reliable constrains during the fitting process, thus the model could not be able to provide reliable descriptions for surface brightness there . These unreliable data will be accounted in the total light measurement and will take up an ineligible fraction(up to 20% according to Sonnenfeld (2020)).However, the traditional definition of galaxy size and mass derived from the best-fit model are both associated with the total light, therefore we believe they are not robust qualities.

Instead of investigating the whole galaxy, we may focus on a fixed, relatively small aperture and investigate some properties inside, following the method proposed in Sonnenfeld (2020). In this work, we choose 10kpc as that aperture,in consideration that it is large enough to enclose sufficient amount of stellar mass while will not be too large to suffer from the extrapolation problem. We use $M_{*,10}$ to denote the mass enclosed inside 10kpc and $\Gamma_{*,10}$ to represent to mass-weighted projected surface density slope.The latter is defined as

$$\Gamma_{*,10} = \frac{2\pi \int_0^{10} R \frac{dlog\Sigma_*}{dlogR} \Sigma_*(R) dR}{2\pi \int_0^{10} R\Sigma_*(R) dR} = 2 - \frac{2\pi \times 10^2 \times \Sigma_*(10)}{M_{*,10}} \quad (1)$$

Assuming a isothermal density profile for elliptical galaxy, the growth in total stellar mass and effective radius due to mergers can be approximated using virial theorem(Naab et al. 2009). In particular, if the mass of one galaxy grow by a factor of η, i.e. $M_f = (1+\eta)M_i$, then the growth of gravititional radius can be expressed as $r_f = \frac{(1+\eta)^2}{(1+\eta\epsilon)} r_i$, here ϵ is the ratio of mean square velocity of the accreted galaxy to that of the progenitor galaxy. . However, switching to $M_{*,10}$ and $\Gamma_{*,10}$ space, it's hard to derive a relation in $\Delta M_{*,10}$ and $\Delta\Gamma_{*,10}$ analytically as a fixed aperture size 10kpc is involved. Nevertheless, N-body simulations can be helpful. We utilize the simulation result from Nipoti et al. (2009) which contains a number of binary mergers with different mass ratio. We measure the $M_{*,10}$ and $\Gamma_{*,10}$ of both progenitor and merger remnant and calculate the growth in these two quantities. In addition to finding that different merger ratio

behaves differently, we also discovered that the scale of galaxy also make diferences.

Having find how the $M_{*,10}$ and $\Gamma_{*,10}$ under different growth scenarios, we then compared them with the evolution of these two quantities in reality. We select ETGs from GAMA DR4 main survey (Galaxy and Mass Assembly, Driver et al. (2022);Bellstedt et al. (2020) ; Baldry et al. (2010); Hopkins et al. (2013)) and obtained precise spectroscopic redshift and other quantities that related to spectrum measurement, e.g. stellar mass. In addition, the structural parameter are measured from KiDs photometry (Kile Degree survey , Kuijken et al. (2019), Roy et al. (2018), Amaro et al. (2021)) using GalNet (Li et al. (2022)). Based on these observation datas, we then calculated their $M_{*,10}$ and $\Gamma_{*,10}$ and further analyse the , $M_{*,10} - \Gamma_{*,10}$ relation and their evolution from $z = 0.6$ to present.

The structure of this paper is as follows. In Sect.2, we give a brief description on both observations from KiDs&GAMA and the binary merger simulation from (Nipoti et al. 2009). I present the result of growth of $M_{*,10}$ and $M_{*,10} - \Gamma_{*,10}$ in different merger scenarios in Sect.3 and present the comparison with observation result in Sect.4. Finally, I give a discussion in Sect.5 then conclude the paper in Sect.6.

In this paper, we assume a flat ΛCDM cosmology with $\Omega_M = 0.3$ and $H_0 = 70km\ s^{-1}\ Mpc^{-1}$. Magnitude are in AB units and stellar mass are in solar units.

2 DATA

2.1 observation sample selection

In this work, we need precise redshift measurment to ensure the stellar mass and aperture size of 10 kpc is accurate. Therefore, we choose to use more reliable spectroscopic redshift instead of photometric redshift, obtaining measurement from ETGs in GAMA DR4. In practise, I use DMU gkvScienceCatv02(Bellstedt et al. (2020)) to select galaxies from GAMA DR4 Main Survey sample, which only inculde galaxies whose r-band magnitude is larger than 19.65 in order to ensure the 95% spec-z completeness of the sample. Further, I obtain the intensity of emission lines from DMU GaussFitSimplev05 (see Gordon et al. (2017)) and obtain the stellar mass measurement from DMU StellarMassesGKVv24(see Driver et al. (2022)). According to Taylor et al. (2011),estimation of stellar mass was done by fitting the Bruzual & Charlot (2003) stellar evolution models with Chabrier (2003) stellar initial mass function (IMF) and the Calzetti et al. (2000) dust curve . In particular, the SEDs was weighted to ensure the model-fitting was operated within a fixed wavelength range (3000 - 11000Å).

In order to select ETGs, we applied a cut on Hβ qeuivalent width: $Ew_{H\beta} < 0$, to exclude galaxies with star-forming activities. In addition, I removed galaxies whose normalised redshift quality $nQ < 2$ following the suggestion by GAMA Collabration((Driver et al. 2022)).

In addition, we exclude galaxies that are not overlapped with KiDs(Kuijken et al. (2019)), in order to utilize the measurement of structural parameters. Here we use **2DPHOT structural parameter catalogue** provided in KiDs DR4 to obtain the Sersic parameters for our sample. In this catalogue, Napolitano use 2dPHOT (La Barbera et al. (2008)) to operate a 1-Sérsic model fitting to KiDs DR4 galaxies using r-band photometry. I further exclude some galaxies with catastrophic measurement such as negative effective radius or stellar mass. Eventually we have 79672 ETGs with measurement of spectroscopic redshift, stellar mass and structural parameters.

2.2 Structural parameter

As is mentioned above, the reason that we do not trust M_* (total stellar mass) and R_e (effective radius) in traditional structural parameters is the fact that they are related with the unreliable data in the outer region of a galaxies which can only be obtained by extrapolate the surface brightness model. However, we believe that best-fitting model is well-constrained by the inner region, and thus it is reasonable to use them describing shape of the surface brightness profile there. In particular, we utilize these structural parameters to calculate $M_{*,10}$ and $\Gamma_{*,10}$, the procedure of which is described in Sect.2.2.2.

2.2.1 Surface brightness model

In our fitting, we use Sérsic profile to model the surface brightness of galaxies :

$$I(R) = I_0 exp\left\{-b_n\left(\frac{R}{R_e}\right)^{1/n}\right\} \tag{2}$$

Here, q is the axis ratio, n is the Sérsic index while R is the circularised radius

$$R^2 = qx^2 + \frac{y^2}{q} \tag{3}$$

where x, y are Cartesian coordinates, located at the center of galaxies. We use symbol x to denote the axis that is aligned with the semi-major axis of the ellipse, while using y to denote axis aligned with semi-minor axis. The effective radius R_e is circularised as well.

Integrating Eq.2, we can obtain the light enclosed in a certain aperture $L(< R)$ (or the total light L_{tot})

$$L(< R) = 2\pi n \cdot I_0 R_e^2 \cdot \frac{1}{(b_n)^{2n}} \cdot \gamma\left[2n, b_n\left(\frac{R}{R_e}\right)^{\frac{1}{n}}\right] \tag{4}$$

$$L_{tot} = 2\pi n \cdot I_0 R_e^2 \cdot \frac{1}{(b_n)^{2n}} \cdot \Gamma(2n) \tag{5}$$

Here Γ is the gamma function, γ is the lower incomplete gamma function and b_n is a constant that ensure the light enclosed within the effective radius R_e is a half of the total light.

$$L_{tot} = 2L(< R_e) \tag{6}$$

Therefore, b_n can be calculated by solving

$$\Gamma(2n) = 2\gamma(2n, b_n) \tag{7}$$

In fact, galaxies may have various component, hence single Sérsic model might not be able to give a accurate description of the entire surface brightness profile. However, as we are focusing on the inner region of the galaxy, our only requirement is just the surface brightness in the inner region of galaxy can be accurately described by model.Therefore, we compared the profile of the enclosed light of galaxies with their best-fitting Sérsic model in Fig 1 . We can easily observe that although some model do have discrepancy at some large radii, the enclosed light within $10kpc$ is still well constrained by model.

2.2.2 $M_{*,10}, \Gamma_{*,10}$ Calculation

In our work, we assume that there is no mass-to-light ratio gradient inside one galaxy, hence the mass profile can be easily obtained via the light profile. We have obtained the stellar mass estimate for each galaxy from GAMA together with the light they use in the SPS

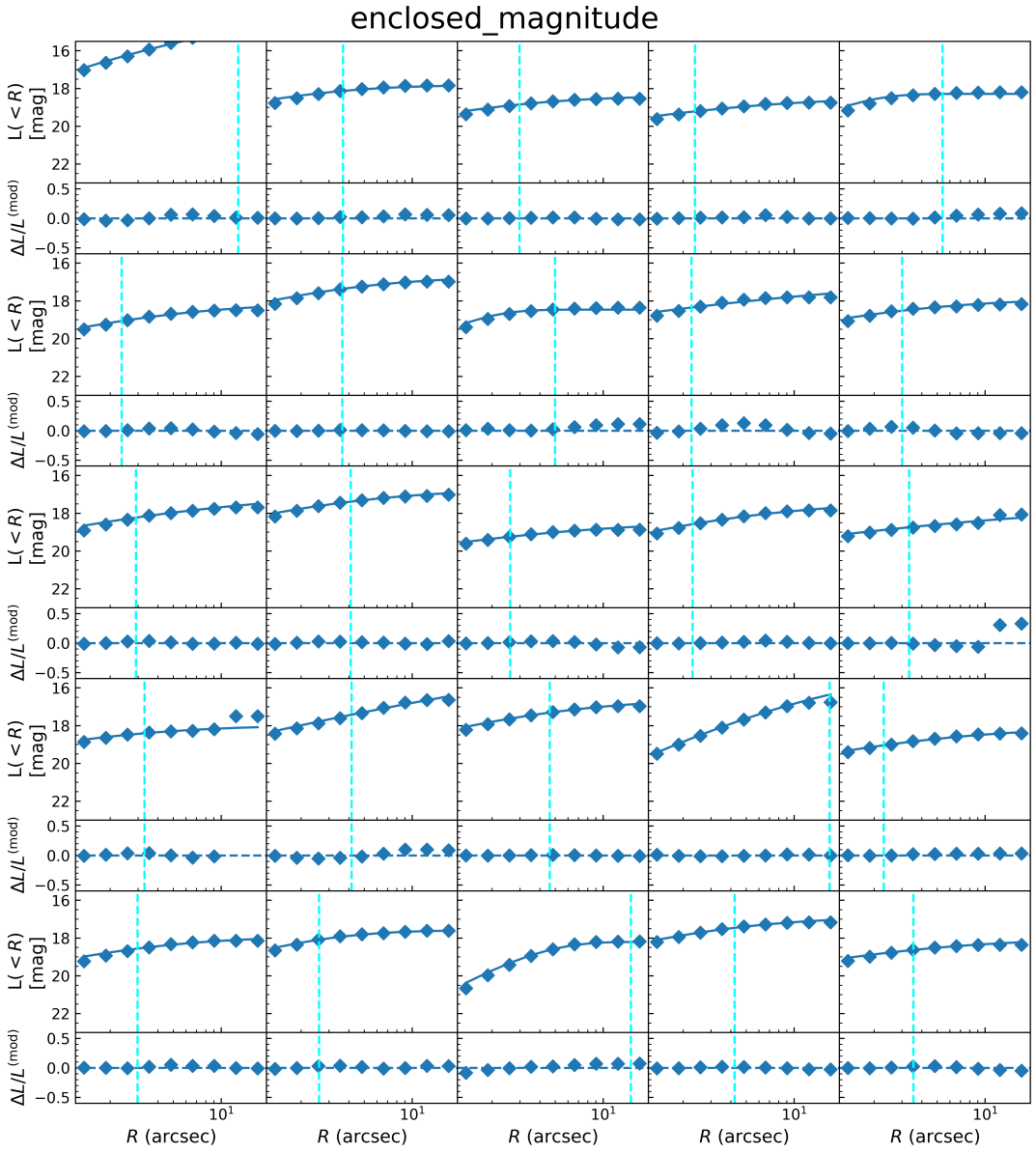

Figure 1. enclosed magnitude

model fitting process (Driver et al. 2022), which enable us to calculate the mass-to-light ratio Υ. The mass profile can be easily obtained by multiplying Eq3 and Eq4 with that Υ.

$$\Sigma_*(R) = \Upsilon I_0 exp\left\{-b_n\left(\frac{R}{R_e}\right)^{1/n}\right\} \tag{8}$$

$$M_*(< R) = \Upsilon 2\pi n \cdot I_0 R_e^2 \cdot \frac{1}{(b_n)^{2n}} \cdot \gamma\left[2n, b_n\left(\frac{R}{R_e}\right)^{\frac{1}{n}}\right] \tag{9}$$

Simply substitute $R = 10kpc$ to Eq9, we obatined $M_{*,10}$, while $\Gamma_{*,10}$ is obatained by substituting Eq8 to Eq1.

2.3 Completeness

To accurately measure the evolution of $M_{*,10}$ and $M_{*,10} - \Gamma_{*,10}$ relation, we do not expect any bias be introduced during the sample selection procedure. Therefore, we need our sample to be complete in $M_{*,10}$. Our fiducial sample is flux-limited, with its 95% completeness limit down to r-band magnitude 19.65. To obtain a $M_{*,10}$ complete sample, we need to translate this completeness limit in magnitude to limit in $M_{*,10}$.

Then we need to translate the r-band critical magnitude $r_{crit} = 19.65$ to one critical $M_{*,10}$, namely $M_{*,10}^{crit}$. In fact, at arbitrary redshift, the ratio between $M_{*,10}$ and the total flux F always spread a relatively wide range. Here we made an assumption that the ratio $M_{*,10}/F$ depend neither on $M_{*,10}$ nor on F, meaning that this quantity only describe one overall nature of quiescent galaxies at one given redshift. We then make narrow redshift bins, calculate the mean and standard deviation of the mass-to-flux ratio $M_{*,10}/F$ and use Gaussian distribution to estimate the critical value $M_{*,10}/F|_{crit}$,where the cumulative probability reach 95% .Mutiplying $M_{*,10}/F|_{crit}$ by the corresponding flux of r_{crit}, we obtained the $M_{*,10}$ limit at that redshift bin.

Fig 2 illustrate the procedure, it shows the dsitribution of $M_{*,10}/F$

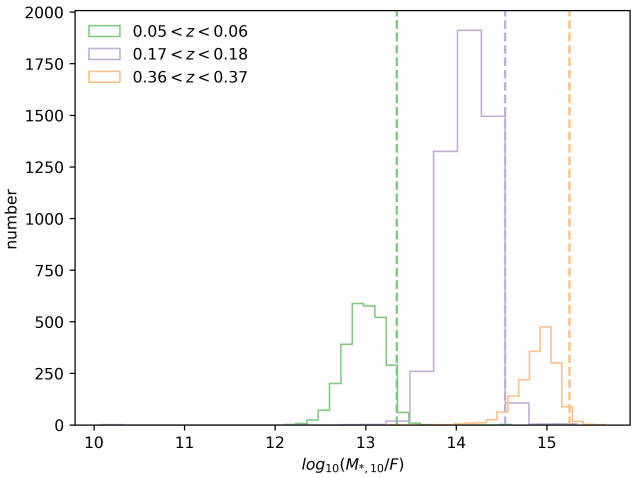

Figure 2. $M_{*,10}$ to flux ratio

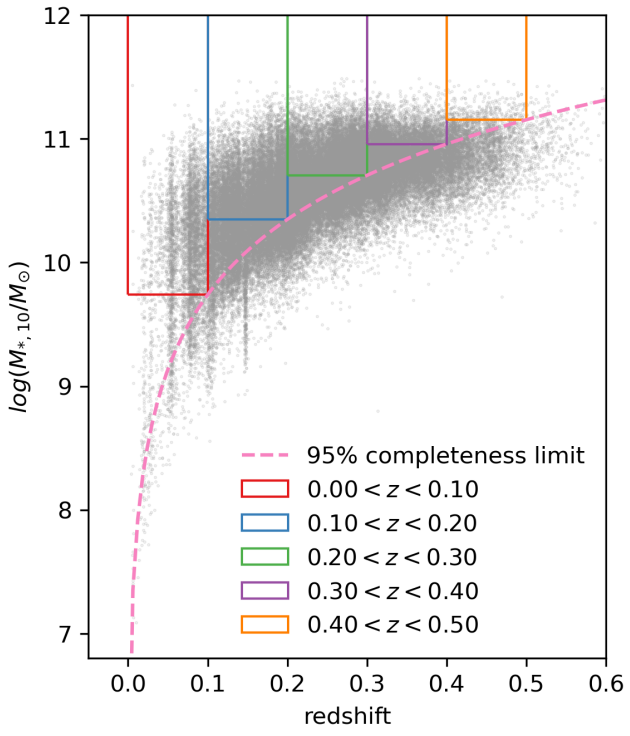

Figure 3. color

in three different redshift bins, with dashed line shows the 95% percentile of each bin. Operate this procedure iterative in each redshift bin and exclude galaxies whose $M_{*,10}$ is lower that the limit, we obtained a sample with 95% completeness in $M_{*,10}$ and is shown in Fig 3

2.4 Simulation

In order to build a intuitive understanding of the growth in $M_{*,10}$ and $\Gamma_{*,10}$ due to mergers, we utilize a collected set of dissipationless binary-merger simulations. For detailed descriptions, one can refer to Sonnenfeld et al. (2014). Here we briefly review some key aspects of the simulation. We have 16 runs in this set with three different merger mass ratios $\xi = 0.2, 0.5, 1.0$. This 16 runs can be divided into two groups by their different behaviour in merging process, namely 'head-on' and 'off-axis' mergers. The pericenter radius $r_{peri} = 0$ for 'head on' mergers while $r_{peri}/r_{vir} \approx 0.2$ for $\xi = 0.2$ and 0.5 and $r_{peri}/r_{vir} \approx 0.4$ for $\xi = 1.0$ for 'off-axis' mergers. Here r_{vir} is the virial radius of the main halo.

3 METHOD

3.1 Random catalogue

Obtaining the $M*_{,10}$ and $\Gamma_{*,10}$ data, we want to plot the $M_{*,10}$ function and investigate its redshift-dependent evolution ,which require us to know the effective volume of our sample. Here we apply the random catalogue method to investigate such issue.....

3.2 Beyesian hierarchical method?

4 RESULT

4.1 $M_{*,10} - \Gamma_{*,10}$ relation and evolution

4.2 Model

REFERENCES

Amaro V., et al., 2021, in Zelinka I., Brescia M., Baron D., eds, , Vol. 39, Intelligent Astrophysics. pp 245–264, doi:10.1007/978-3-030-65867-0_11
Baldry I. K., et al., 2010, MNRAS, 404, 86
Belli S., Newman A. B., Ellis R. S., 2015, apj, 799, 206
Bellstedt S., et al., 2020, Monthly Notices of the Royal Astronomical Society, 496, 3235
Bruzual G., Charlot S., 2003, Monthly Notices of the Royal Astronomical Society, 344, 1000
Calzetti D., Armus L., Bohlin R. C., Kinney A. L., Koornneef J., Storchi-Bergmann T., 2000, apj, 533, 682
Carollo C. M., et al., 2013, The Astrophysical Journal, 773, 112
Chabrier G., 2003, pasp, 115, 763
D'Eugenio F., et al., 2023, Evolution in the Orbital Structure of Quiescent Galaxies from MAGPI, LEGA-C and SAMI Surveys: Direct Evidence for Merger-Driven Growth over the Last 7 Gy (arxiv:2303.05520)
Daddi E., et al., 2005, The Astrophysical Journal, 626, 680
Damjanov I., Zahid H. J., Geller M. J., Utsumi Y., Sohn J., Souchereau H., 2019, The Astrophysical Journal, 872, 91
Dekel A., Burkert A., 2014, Monthly Notices of the Royal Astronomical Society, 438, 1870
Dokkum P. G. v., Franx M., 1996, Monthly Notices of the Royal Astronomical Society, 281, 985
Driver S. P., et al., 2022, MNRAS, 513, 439
Fagioli M., Carollo C. M., Renzini A., Lilly S. J., Onodera M., Tacchella S., 2016, The Astrophysical Journal, 831, 173
Fan L., Lapi A., De Zotti G., Danese L., 2008, The Astrophysical Journal, 689, L101
Gordon Y. A., et al., 2017, mnras, 465, 2671
Hamadouche M. L., et al., 2022, Monthly Notices of the Royal Astronomical Society, 512, 1262
Hilz M., Naab T., Ostriker J. P., 2013, Monthly Notices of the Royal Astronomical Society, 429, 2924
Hopkins P. F., Bundy K., Hernquist L., Wuyts S., Cox T. J., 2010, Monthly Notices of the Royal Astronomical Society, 401, 1099
Hopkins A. M., et al., 2013, MNRAS, 430, 2047
Kuijken K., et al., 2019, Astronomy & Astrophysics, 625, A2
La Barbera F., de Carvalho R. R., Kohl-Moreira J. L., Gal R. R., Soares-Santos M., Capaccioli M., Santos R., Sant'Anna N., 2008, pasp, 120, 681
Li R., Napolitano N. R., Roy N., Tortora C., La Barbera F., Sonnenfeld A., Qiu C., Liu S., 2022, The Astrophysical Journal, 929, 152
Naab T., Johansson P. H., Ostriker J. P., 2009, The Astrophysical Journal, 699, L178
Newman A. B., Ellis R. S., Bundy K., Treu T., 2012, The Astrophysical Journal, 746, 162
Nipoti C., Treu T., Bolton A. S., 2009, The Astrophysical Journal, 703, 1531
Oser L., Naab T., Ostriker J. P., Johansson P. H., 2011, The Astrophysical Journal, 744, 63
Roy N., et al., 2018, MNRAS, 480, 1057
Sonnenfeld A., 2020, A&A, 641, A143
Sonnenfeld A., Nipoti C., Treu T., 2014, The Astrophysical Journal, 786, 89
Tal T., van Dokkum P. G., 2011, apj, 731, 89
Taylor E. N., et al., 2011, mnras, 418, 1587
Toft S., et al., 2007, The Astrophysical Journal, 671, 285
Trujillo I., et al., 2006, Monthly Notices of the Royal Astronomical Society, 373, L36
Trujillo I., Conselice C. J., Bundy K., Cooper M. C., Eisenhardt P., Ellis R. S., 2007, Monthly Notices of the Royal Astronomical Society, 382, 109
van Dokkum P. G., Brammer G., 2010, apjl, 718, L73
van Dokkum P. G., Franx M., 2001, The Astrophysical Journal, 553, 90
van Dokkum P. G., et al., 2008, The Astrophysical Journal, 677, L5
van Dokkum P. G., et al., 2010, The Astrophysical Journal, 709, 1018
van der Wel A., et al., 2014, The Astrophysical Journal, 788, 28

This paper has been typeset from a TEX/LATEX file prepared by the author.